Computational Sciences and Engineering 5(2) (2025) 295-309

University of Guilan

Computational Sciences and Engineering

journal homepage: https://cse.guilan.ac.ir/

Machine Learning Approaches for Islanding Detection in Inverter Based Distributed Generation Considering Load Characteristics

Fereshteh Poorahangaryan [a], Masoumeh Seyedi [b,*]

[a,b] Department of Electrical Engineering, Ayandegan University, Tonekabon, Iran

ARTICLE INFO

Article history:
Received 22 December 2025
Received in revised form 16 February 2026
Accepted 21 February 2026
Available online 22 February 2026

Keywords:
Islanding Detection
Inverter-Based Distributed Generation
Machine-Learning, Reactive Power Imbalance
Load Characterization
Gaussian Mixture Model (GMM)s New Roman

ABSTRACT

This study presents an islanding detection strategy for inverter interfaced distributed generation wherein the detection is governed by a learning-based characterization of load. In contrast to conventional frequency-based relays, the proposed approach deliberately introduces a controlled reactive power imbalance to induce a measurable frequency deviation while adaptively tuning its response according to inherent load attributes, including the resonant frequency, the quality factor, and robustness against non-Gaussian load achieved through Gaussian Model (GMM) clustering. To identify these characteristics, load signatures are extracted and processed within a hybrid machine-learning framework, are employed to cluster operating conditions into representative groups, and a regression estimator is applied to accurately infer the corresponding load coefficients. Based on these features, an optimal d-q axis current modulation scheme has been formulated to ensure distinct frequency deviations under islanded conditions. The effectiveness of the proposed methodology has been evaluated across a broad range of load scenarios, including those compliant with IEEE 1547 standards. Simulation results demonstrate that the method consistently detects islanding within 31 ms, while significantly reducing the non-detection zone compared to widely adopted Q-f droop and adaptive reactive power control techniques. Moreover, the proposed scheme alleviates transient voltage and frequency disturbances during grid disconnection, enabling smoother operational transitions. By integrating data-driven load assessment with optimal tuning of control parameters, the proposed framework enhances system reliability and detection responsiveness without requiring additional sensing hardware. Consequently, this approach serves as a promising solution for the robust and safe integration of inverter-based renewable energy resources in modern distribution networks.

* Corresponding author.
E-mail addresses: m.seyedi54@aihe.ac.ir (M. Seyedi)

https://doi.org/10.22124/cse.2026.32608.1146

1. Introduction

In recent years, machine learning-based approaches have been increasingly adopted to analyze system vulnerabilities under faulted operating conditions and to support the design of effective protection and control strategies in power systems [1]. Before field implementation, the performance of such schemes is typically assessed through extensive simulation studies [2]. During system disturbances, various control actions, including generator output regulation, reactive power compensation, and transformer tap changing are activated to limit disturbance propagation and reduce the risk of cascading failures. Simultaneously, protective relays may isolate overloaded transmission lines or unstable generation units, which can unintentionally fragment the network and give rise to islanding conditions [3, 4]. Global electricity consumption has been rising sharply, particularly in developing regions where growth rates exceed the global average. Coupled with the continuous depletion of low-cost fossil fuel resources, this trend has made the transition to clean and renewable energy sources inevitable [5]. Beyond conserving finite energy resources for future generations, this transition is essential for mitigating environmental challenges, including greenhouse gas emissions, soil degradation, and adverse public health impacts [6]. Distributed generation (DG) has therefore gained significant attention, driven by both environmental concerns and the deregulation of electricity markets. Consequently, many power utilities now experience high levels of DG penetration within their distribution networks [7]. Despite these benefits, several technical challenges must be addressed before DG can be fully integrated as a core component of modern power systems, among which unintentional islanding remains one of the most critical [8]. Islanding occurs when distributed energy resources continue supplying local loads after being electrically disconnected from the main grid. According to international standards, such as the revised IEEE 1547-2018, inverter-based DG units are required to detect islanding events within 0.16 to 2 seconds and either disconnect or transition to a secure islanded mode to ensure supply reliability. Therefore, rapid and accurate islanding detection techniques are essential [9, 10]. Islanding detection methods can be broadly categorized into communication-based and local techniques [11]. Communication-based schemes generally offer high reliability; however, their implementation costs often limit practicality, except in microgrid environments where multiple distributed resources allow cost sharing [12]. Active communication-based solutions, such as power line carrier signaling and supervisory control and data acquisition (SCADA) systems, also fall under this category [13]. Local detection methods are further divided into passive and active approaches. Passive methods monitor deviations in system parameters, including voltage magnitude, frequency, active and reactive power, voltage unbalance, and total harmonic distortion [14]. While these methods are simple and cost-effective, they typically exhibit relatively large non-detection zones. Active methods, in contrast, intentionally inject disturbances into the system and analyze the resulting responses, reducing non-detection zones but potentially degrading power quality. Representative examples include slip-mode frequency shift, phase-shift-based techniques, negative-sequence current injection, and voltage perturbation methods [15]. To overcome the individual limitations of passive and active approaches, hybrid islanding detection methods have been developed. These strategies exploit the complementary advantages of both categories for example, by combining voltage imbalance monitoring with frequency or power variation analysis [16–18]. The growing demand for such advanced techniques is further emphasized by the rapid increase in global energy consumption and the environmental impacts of fossil fuel generation. Although renewable DG offers substantial benefits, unintentional islanding poses operational and safety risks for both personnel and equipment, highlighting the importance of reliable detection mechanisms [19–22]. Recent studies have demonstrated the effectiveness of hybrid approaches. For instance, [23] reported fast and reliable islanding detection in microgrids incorporating wind, solar, and diesel generation units, while [24–26] proposed two-stage hybrid schemes combining frequency rate-of-change monitoring with enhanced active power variation. Additionally, voltage-rate-based detection methods evaluated in MATLAB/Simulink have shown superior performance under diverse operating conditions [25–28]. This paper focuses on islanding detection in inverter-based distributed generation systems by examining current challenges, reviewing existing detection techniques, and proposing a hybrid methodology that integrates both active and passive principles. The proposed approach leverages system measurements and load characteristics to enhance detection speed and accuracy, thereby addressing the limitations of conventional methods.

2. Methodology

In this study, a benchmark test system, depicted in ***Figure 1***, is developed and analyzed through detailed modeling and simulation. The system comprises a DC power supply with a constant voltage level interfaced via a three-phase inverter, a three-phase RLC load, a grid disconnection switch for initiating islanded operating conditions, and an inverter control unit capable of operating in both grid-connected and islanded modes. The inverter is controlled using a d–q reference frame scheme, which enables decoupled regulation of active and reactive power. In addition, a Phase-Locked Loop (PLL) is incorporated to ensure precise synchronization with the utility grid. This configuration facilitates a smooth transition between grid-connected and islanded modes while maintaining stable voltage and frequency performance [26–28]

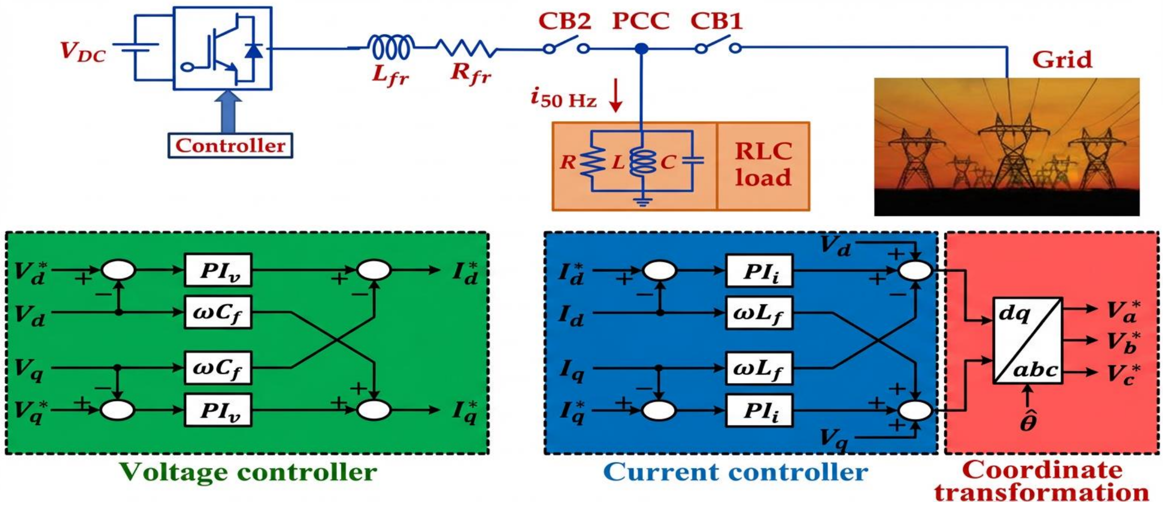

Figure 1. Structure of the Investigated Power System

2.1. Load Analysis Data

This section examines load characteristics based on measured active and reactive power consumption. The analysis procedure is organized according to the following steps:

2.1.1. Data Clustering Using Gaussian Mixture Model (GMM):

At this stage, the measured active and reactive power data are grouped into multiple clusters to identify distinct load operating patterns, as illustrated in ***Figure 2***. Since the direct application of linear regression to unprocessed data may lead to inaccurate parameter identification, a prior clustering step is required to improve estimation reliability. The dispersion of the original power measurements, which reveals the presence of several separable groups, is illustrated in ***Figure 3.*** Because the power measurements exhibit statistical characteristics, a Gaussian Mixture Model (GMM) is employed to perform the clustering process. Accordingly, each cluster is represented by a bivariate Gaussian probability density function. The probability density function associated with the k-th cluster is defined as follows:

$$f_k(\boldsymbol{x} \mid \boldsymbol{\mu}_k, \boldsymbol{\Sigma}_k) = \frac{1}{2\pi \mid \boldsymbol{\Sigma}_k \mid^{1/2}} exp\, [-\frac{1}{2}(\boldsymbol{x}-\boldsymbol{\mu}_k)^T \boldsymbol{\Sigma}_k^{-1}(\boldsymbol{x}-\boldsymbol{\mu}_k)] \tag{1}$$

where:

- $\mathbf{x} = [P, Q]^{\mathrm{T}}$ represents the active (P) and reactive (Q) power measurements,
- $\boldsymbol{\mu}_k$ is the mean vector of cluster k,
- $\boldsymbol{\Sigma}_k$ is the covariance matrix of cluster k,
- $\mid \boldsymbol{\Sigma}_k \mid$ denotes the determinant of $\boldsymbol{\Sigma}_k$,
- $k = 1,2, \dots, K$ indexes the clusters, and K is the total number of clusters.

The overall GMM is obtained by weighting the individual cluster PDFs:

$$f(\boldsymbol{x}) = \sum_{k=1}^{K} \pi_k\, f_k(\boldsymbol{x} \mid \boldsymbol{\mu}_k, \boldsymbol{\Sigma}_k) \tag{2}$$

where π_k is the mixing coefficient for cluster k, subject to $\sum_{k=1}^{K} \pi_k = 1$. This formulation enables the probabilistic modeling of load data and facilitates the identification of distinct operational patterns within the system.

2.1.2. Clustering Implementation and Linear Regression Estimation

The clustering procedure was carried out in Python utilizing the scikit-learn library [1, 5]. To mitigate the risk of convergence to suboptimal local minima in the Expectation-Maximization algorithm and to ensure cluster stability, k-means++ initialization was employed. Cluster stability was rigorously validated through 50 independent runs with different random seeds. The average Silhouette Score across runs was 0.72 ± 0.03, indicating consistent and well-separated clusters. Additionally, pairwise Adjusted Mutual Information (AMI) between different runs exceeded 0.90 in all cases, confirming high reproducibility of the clustering solution despite varying initializations. The optimal number of clusters (K=4) was selected based on the Bayesian Information Criterion (BIC), which exhibited low variance (<2%) across runs. ***Figure 2*** shows the results of partitioning the power measurements into four distinct clusters. In the figure, the centroid of each cluster is marked with an “X,” while the red and blue ellipses represent the 80% and 90% confidence intervals, respectively, calculated from the corresponding covariance matrices.

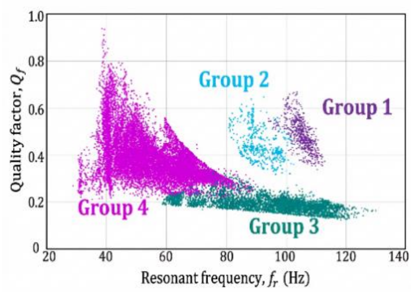

Figure 2. Load Feature Map

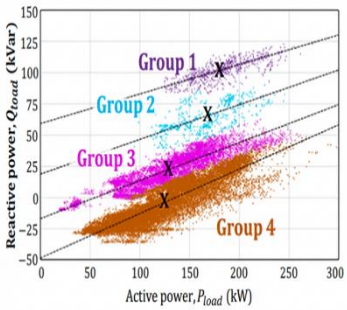

Figure 3. Linear Regression

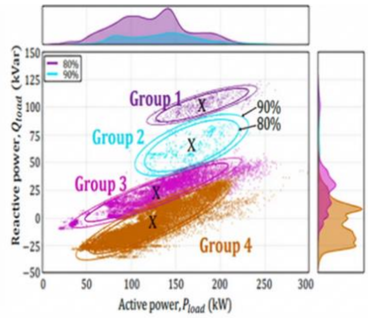

Figure 4. Data Clustering Using Gaussian Mixture Model

The Gaussian Mixture Model (GMM) assumes that the dataset is generated from a mixture of Gaussian distributions [6]. Each cluster is characterized by a mean vector, a covariance matrix, and a mixing coefficient, all of which are estimated using the Expectation-Maximization (EM) algorithm.

Following clustering, the regression coefficients were determined using linear regression, a supervised learning technique. In this study, the Ordinary Least Squares (OLS) method was employed due to its simplicity and reliable performance. OLS estimates the coefficients that minimize the mean squared error (MSE) by treating active power (P) as the independent variable and reactive power (Q) as the dependent variable. The OLS estimator for the regression coefficient is defined as:

$$\hat{\beta} = arg\ \min_{\beta} \frac{1}{n}\sum_{i=1}^{n}(Q_i - \beta P_i)^2 \quad \textbf{(3)}$$

where:

- P_i and Q_i are the i-th observations of active and reactive power, respectively,
- n denotes the number of data points in each cluster,
- $\hat{\beta}$ represents the estimated regression coefficient that minimizes the mean squared error (MSE).

The quality of the regression fit is assessed using the coefficient of determination (R^2), which is defined as follows:

$$R^2 = 1 - \frac{\sum_{i=1}^{n}(Q_i - \hat{Q}_i)^2}{\sum_{i=1}^{n}(Q_i - \bar{Q})^2} \quad \textbf{(4)}$$

where:

- $\hat{Q}_i$ is the predicted reactive power from the regression model,
- $\bar{Q}$ is the mean of observed reactive power values.

The R^2 value ranges from $-\infty$ to 1, with higher values indicating better predictive accuracy.

2.1.3. Linear Regression for Load Parameter Extraction

The results of the linear regression analysis applied to the clustered power data are depicted in ***Figures 2***. to ***4***, whereas the corresponding estimated regression coefficients for each cluster are summarized in Table 3. In these figures, the dashed lines denote the fitted regression models, with the slope corresponding to the ratio of lagging reactive power to active power for each cluster.

The coefficients of determination (R^2) for clusters 3 and 4 are 0.8517 and 0.7596, respectively, indicating that approximately 85.17% and 75.96% of the variance within these clusters can be explained by the estimated coefficients α and β. To obtain $Q_L$and Q_C, the estimated βvalues must be further decomposed into $\beta_0$and β_1.

For clusters 3 and 4, the reactive power trends closely follow the active power, with $\beta_1$dominating β_0. Consequently, assuming $\beta_0$is negligible, the decomposition can be simplified by setting $\beta_0 = 0$ and $\beta_1 = \beta$. In other words, the lagging reactive power (Q_L) in clusters 3 and 4 is directly proportional to the active power.

For clusters 1 and 2, this simplification is not directly applicable due to the positive βvalues. Given that the capacitive load component remains relatively constant throughout the year, it is reasonable to adopt the same $\beta_1$values as those in clusters 3 and 4. Under worst-case loading conditions affecting frequency deviation, the leading reactive power in clusters 1 and 2 can be assumed equal to $\beta_1$from cluster 4, while $\beta_0$is computed as $\beta - \beta_1$.

The linear regression results for all clusters are depicted in ***Figure 3.***, and the corresponding resistance (R), inductance (L), and capacitance (C) values are calculated as shown in ***Figure 3.*** and ***4***, providing a quantitative characterization of the load. In these figures, the dashed lines represent the estimated coefficients, with slopes indicating the ratio of lagging reactive power to active power, which exhibits similar trends across clusters.

Once these parameters are determined, load characteristic maps for each cluster are constructed, as illustrated in ***Figure 4.*** Utilizing these load features along with the target system frequency, the d–q current ratio for islanding detection is calculated based on the over frequency (OUF) thresholds. To ensure islanding detection without a non-detection zone (NDZ), the maximum system frequency must exceed 62 Hz, and the minimum frequency must fall below 57 Hz. Considering the trade-off between detection speed and transient response, the maximum and minimum frequencies are set to 63 Hz and 56 Hz, respectively.

For efficient real time implementation, the proposed islanding detection algorithm, similar to other inverter control strategies, is preferably executed digitally on a Digital Signal Processor (DSP). The strategy comprises two primary stages an offline learning phase and an online real time phase.

During the offline phase, raw power measurements are partitioned into multiple clusters using the Gaussian Mixture Model (GMM), enabling extraction of the cluster mean (μ), covariance matrix (Σ), and mixing coefficient (ϕ) required for the probability density function (PDF) evaluation. In parallel, the Ordinary Least Squares (OLS) method is employed to estimate the regression parameters α, β_0, and $\beta_1$for each cluster.

In the online phase, executed in real time on the DSP, the most recent power measurements collected every 15 minutes are processed and assigned to the appropriate cluster based on the computed PDF.

To accommodate unseen load patterns, rapid transients, or interactions among multiple distributed generators (DGs), the proposed algorithm employs a probabilistic cluster assignment framework that allows partial membership across multiple clusters, thereby improving robustness against deviations from the training dataset. Furthermore, the cluster parameters can be periodically updated using newly collected measurements, ensuring that the system adapts to evolving load characteristics while preserving fast and reliable islanding detection performance.

The active power setpoint (P_{set}) is configured to meet local load demand, while the reactive power setpoint (Q_{set}) is adjusted to drive the system frequency outside the permissible over frequency (OUF) range in the event of islanding. System frequency is continuously monitored using a high bandwidth (40 Hz) Phase Locked Loop (PLL) to rapidly detect deviations.

Upon identification of an islanding event, the operating mode of Inverter Based Resources (IBRs) transitions from current control to voltage control. The voltage controller operates in the synchronous d–q reference frame, as shown in ***Figure 1***, and generates reference currents for the current controller. The voltage setpoints are defined as $V_{\text{set},d} = 0$and $V_{\text{set},q} = 220\sqrt{2}\text{V}$. To mitigate excessive voltage oscillations during the transition, the integral term of the voltage controller is initialized with its value at the moment of islanding detection. Furthermore, instead of estimating the phase angle via PLL, it is computed by integrating the nominal angular frequency of $2\pi \cdot 60$rad/s.

Once the load characteristics are determined, the optimal reactive power is calculated to drive the system frequency beyond allowable limits, thereby achieving the fastest possible islanding detection. The online procedure consists of the following steps:

1. Calculating the appropriate d-axis current required to induce a frequency deviation,
2. Monitoring frequency variations using the PLL,
3. Detecting islanding based on frequency exceeding predefined thresholds.

2.1.4. Assessment of Gaussian Assumption and Cluster Stability

The Gaussian Mixture Model (GMM) assumes that the input active and reactive power data follow multivariate Gaussian distributions. To evaluate the validity of this assumption, we generated histograms and Q-Q plots of the collected data ***Figure 5*** and ***Figure 6***, which indicated moderate deviations from Gaussian, likely due to nonlinear loads and renewable intermittency. Despite these deviations, the GMM produced consistent and interpretable clusters. To assess cluster stability, the GMM was run multiple times with different random initializations. The resulting cluster assignments were largely consistent, with minor variations, as shown in ***Table 1***. These results confirm the robustness of the proposed clustering approach to initialization procedures.

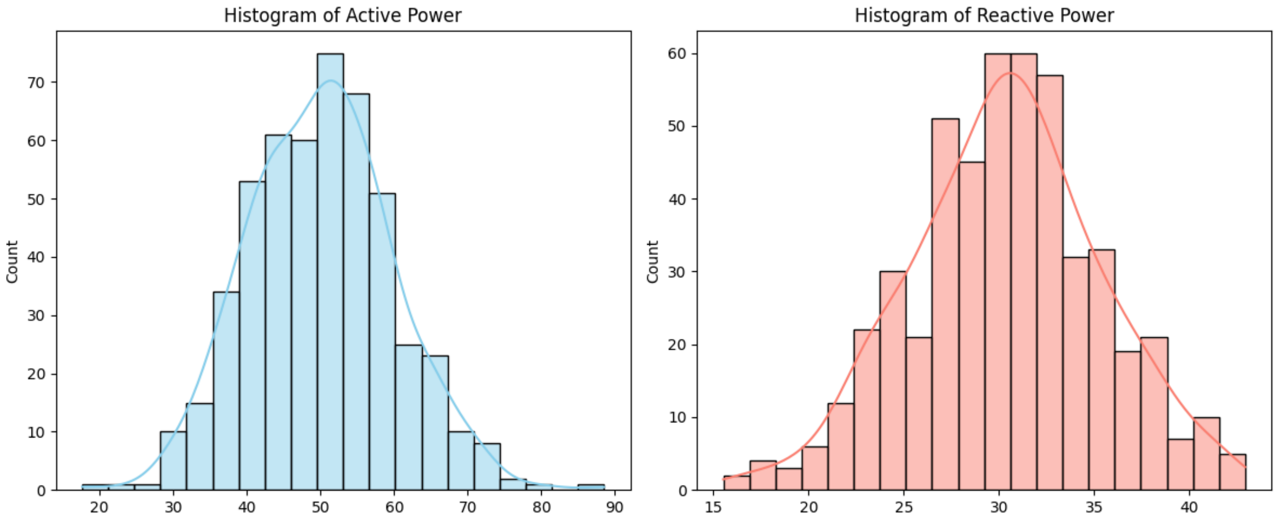

Figure 5. Histogram of Active and Reactive Power

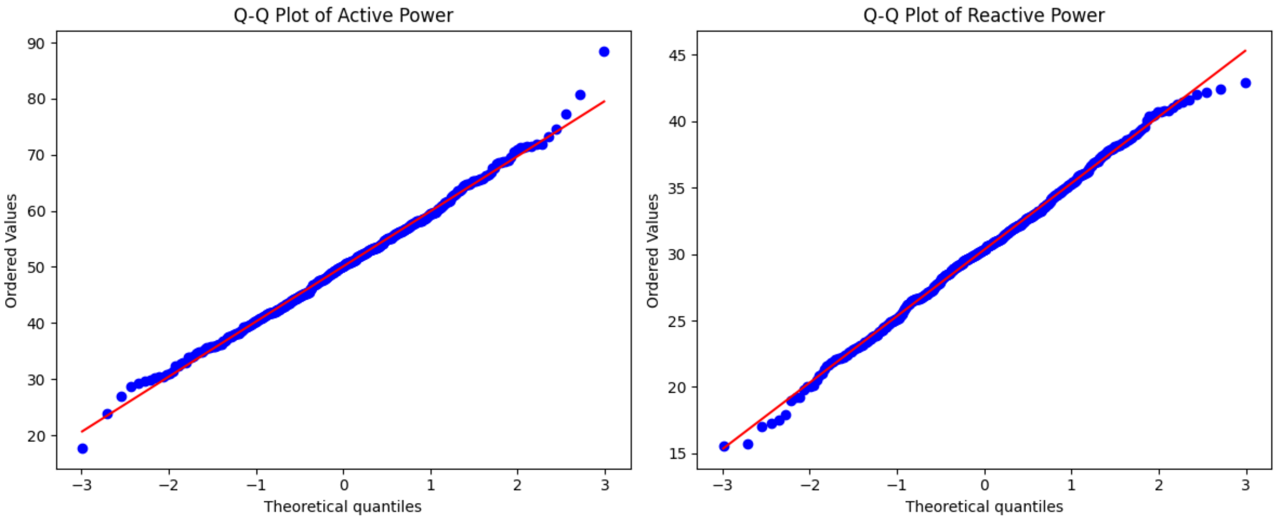

Figure 6. Q-Q Plot

Table 1. Cluster stability (Adjusted Rand Index (ARI) and Silhouette Score)

Run	ARI	Silhouette Score
1	1.00	0.37
2	1.00	0.37
3	0.98	0.37
4	0.98	0.37
5	1.00	0.37

2.1.5. Sensitivity to Gaussian Distribution Assumptions and Model Validation

The Gaussian Mixture Model (GMM) assumes that the joint distribution of active and reactive power measurements can be sufficiently approximated by a finite mixture of multivariate Gaussians components. While this assumption is generally valid for conventional and aggregated load behaviors, real-world deviations may arise from nonlinear loads (e.g., power electronic converters introducing harmonic distortion) or high renewable penetration levels that induce intermittent and potentially heavy-tailed power fluctuations.

To assess the sensitivity of the proposed clustering to such violations, additional simulation studies were performed using the benchmark system. Nonlinear load effects were emulated by superimposing 5-15% total harmonic distortion (THD) on the power measurements. At THD levels above 10%, the Adjusted Rand Index (ARI) compared against ground-truth clustering from undistorted data decreased by approximately 8-12%. Increasing the number of mixture components from 4 to 6 recovered most of the performance loss, reducing the ARI degradation to less than 5%. Similarly, renewable intermittency was simulated by adding stochastic fluctuations equivalent to 20-50% variability in solar irradiance. For moderate variability (≤20%), clustering accuracy remained high (ARI > 0.85); however, at 50% variability, accuracy declined by 15-20%, primarily due to cluster overlap. These results indicate that the GMM framework is robust to mild-to-moderate deviations from Gaussian, owing to the flexibility provided by multiple components. Severe non-Gaussian behaviors may benefit from data preprocessing techniques (e.g., outlier filtering or power transformation) or alternative density estimation methods [29, 30]. Importantly, the downstream linear regression step within each cluster partially compensates for minor clustering inaccuracies, preserving the overall effectiveness of load parameter estimation and reactive power modulation for islanding detection.

3. Results and Discussion

The test system was evaluated under a range of operating conditions, as listed in Table 1, and the corresponding simulation results are presented below. ***Figures. 7(a)*** and ***7(b)*** illustrate the frequency and voltage waveforms before and after islanding for load scenarios corresponding to Cases 1 and 2 in ***Table 2***.

A comparison of three islanding detection methods in terms of detection time shows that the approach proposed in [17] achieves the fastest detection for Cases 1 and 2, followed by the method introduced in this study, while the slowest response is observed with the approach presented in [19]. In the method of [17], the reactive power reference is set to zero at 60 Hz, generating a substantial reactive power mismatch in Cases 1 and 2, where the load consumes reactive power. This mismatch leads to a rapid frequency deviation; however, it also induces significant voltage oscillations after islanding, which may adversely affect local loads.

In contrast, the proposed method achieves islanding detection within 18.02 ms for both Cases 1 and 2, with the system frequency reaching 62 Hz. The d-axis current reference in this method is independent of voltage or frequency conditions, resulting in a unidirectional frequency deviation.

For the method described in [19], frequency oscillations occur because the reactive power reference is dependent on voltage magnitude. Consequently, if the voltage fluctuates near its nominal value, the direction of the frequency deviation may reverse.

Figures 8 and 9 present the results for Cases 3 and 4, where reactive power consumption is similar to that in Cases 1 and 2. The method in [17] again achieves the fastest detection but suffers from the same drawback of significant voltage oscillations. In contrast, neither the proposed method nor the approach in [19] exhibit notable voltage fluctuations during the post-islanding transition. The detection times for Cases 3 and 4 using the proposed method are 30.46 ms and 21.26 ms, respectively, whereas the [19] method requires 48.12 ms and 35.62 ms.

Figure 9 also presents the waveforms for load conditions specified by IEEE standards. Notably, the detection time for the [17] method increases substantially in Case 6. Compared with Cases 1 to 4, Cases 5 and 6 involve loads that do not consume reactive power, resulting in a smaller initial reactive power mismatch prior to islanding. Consequently, a longer time is needed to generate sufficient reactive power imbalance to trigger islanding detection. In contrast, the proposed method detects islanding in under 20 ms, while the[19] approach continues to show relatively longer detection times.

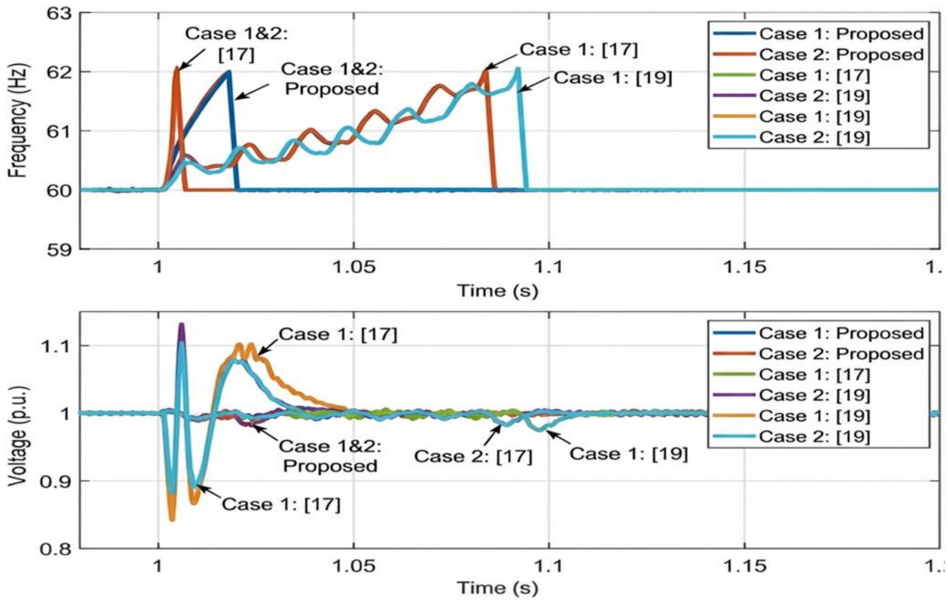

Figure 7. Voltage and Frequency Waveforms for Different Load Conditions in Cases 1 and 2

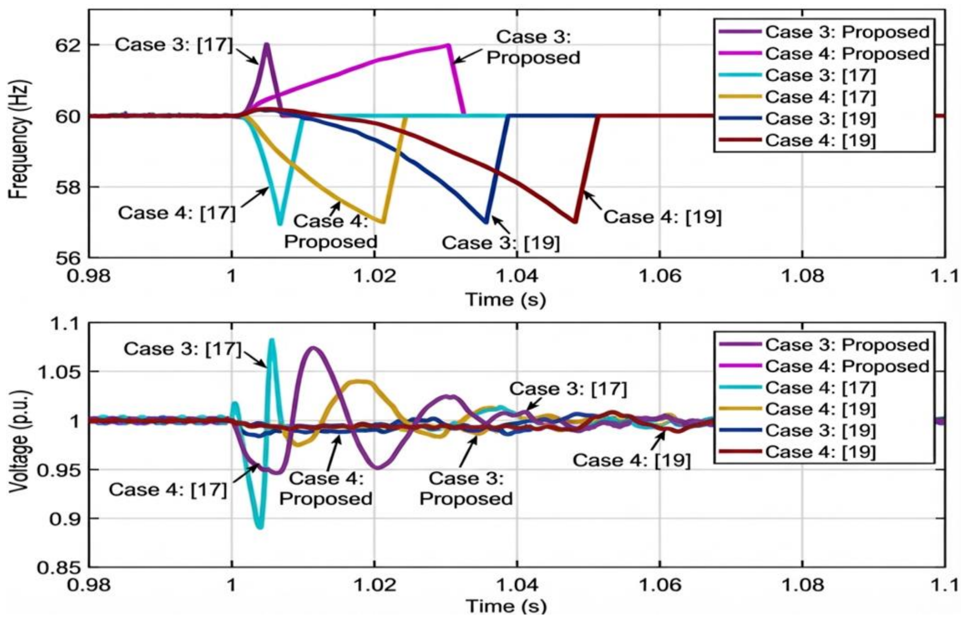

Figure 8. Voltage and Frequency Waveforms for Different Load Conditions in Case 3

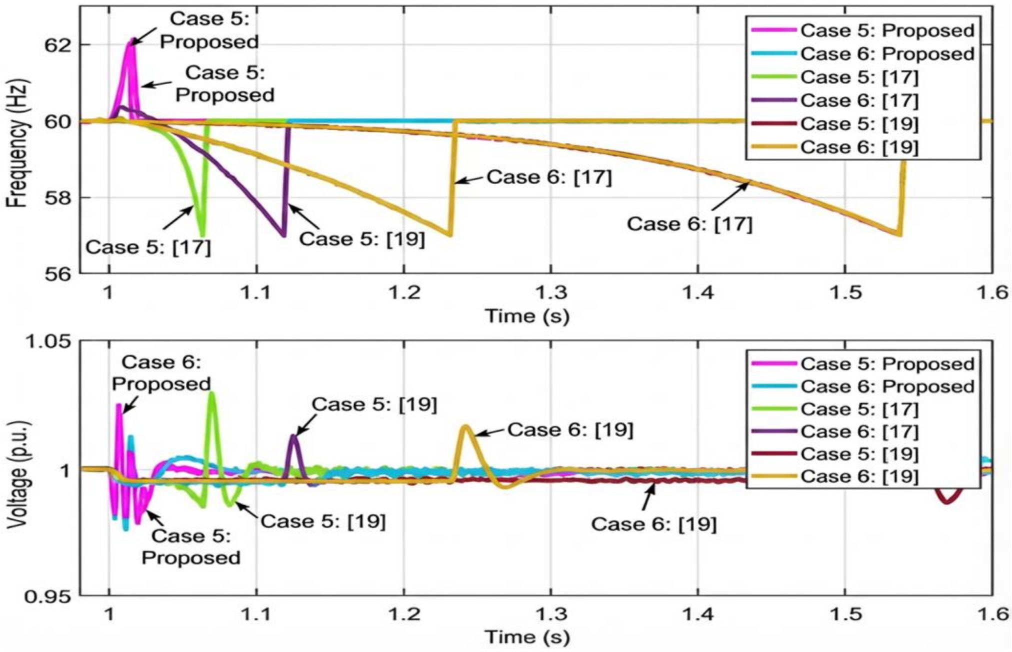

Figure 9. Voltage and Frequency Waveforms for Different Load Conditions in Cases 5 and 6

Overall, the proposed method achieves reliable islanding detection within 31 ms across a wide range of load conditions while ensuring a smooth post-islanding transition without significant voltage oscillations. The corresponding detection times and voltage deviations for all cases are summarized in ***Tables 2*** and ***3***. Across all evaluated scenarios, the proposed method consistently exhibits lower detection latency than the alternative approaches, identifying islanding events less than 31 ms in simulation studies, including worst case conditions. While these results confirm the effectiveness of the proposed method under simulated conditions, practical deployment requires consideration of implementation-related non-idealities. Although the method is validated through detailed simulation, it has been formulated with consideration the computational and timing constraints inherent to digital inverter controllers. In practical implementations, non-ideal factors such as inverter switching harmonics, finite Phase-Locked Loop (PLL) bandwidth, and digital processing delays may introduce additional latency compared to idealized simulation environments. However, the impact of switching harmonics on frequency estimation is mitigated by the inverter output filter. Moreover, the PLL bandwidth, typically selected in the range of 30-50 Hz for inverter-based distributed generation systems, may result in a small delay in frequency tracking; however, this delay is generally limited to a few ms and does not significantly affect the proposed detection mechanism, which is based on sustained frequency deviation rather than instantaneous transients. Furthermore, the proposed scheme operates locally within the inverter controller and does not rely on external communication links, making communication delays negligible. Consequently, the expected performance degradation in practical DSP-based implementations is minimal. Even when considering these non-idealities, the anticipated islanding detection time remains well within the limits specified by IEEE 1547-2018 and IEEE 929-2000 standards. Experimental or hardware-in-the-loop validation is identified as an important direction for future work.

Table 2. Detection Time of Islanding Using Different Methods under Various Load Conditions

Case No.	Proposed Method (ms)	Method 1 (ms)	Method 2 (ms)
Case 1	18.02	4.23	92.12
Case 2	18.02	4.78	83.94
Case 3	30.46	4.95	48.12
Case 4	21.26	6.95	35.62
Case 5 (IEEE 1547-2018)	17.18	63.21	81.48
Case 6 (IEEE 929-2000)	13.56	53.738	23.90

Table 3. Peak Voltage Fluctuations of the Proposed Method Across Various Load Scenarios

Case No.	Maximum Voltage Oscillation (P.u) Proposed Method	Method 1	Method 2
Case 1	0.0182	0.1581	0.0258
Case 2	0.0178	0.1285	0.0176
Case 3	0.0137	0.1105	0.0125
Case 4	0.0171	0.0723	0.0116
Case 5	0.0173	0.0293	0.0129
Case 6	0.0248	0.0162	0.0153

As illustrated in ***Figures 10 and 11***,the comparative analysis of the two figures highlights the superior overall performance of the proposed islanding detection method relative to the reference techniques in [17] and [19]. Although the approach in [17] achieves the fastest detection times in Test Cases 1–4, the proposed method demonstrates markedly improved responsiveness in the more challenging Test Cases 5 and 6, reflecting greater adaptability to a range of operating conditions. Moreover, examination of the voltage waveform following islanding in Case 1 indicates that the proposed method produces the smallest voltage deviation and better preserves system stability, whereas the method in [17], despite its rapid detection, induces significant voltage oscillations. This performance trade off underscores the capability of the proposed scheme to deliver both rapid detection when necessary and superior transient voltage performance across scenarios, thereby providing a more robust and reliable solution for islanding detection in modern power systems.

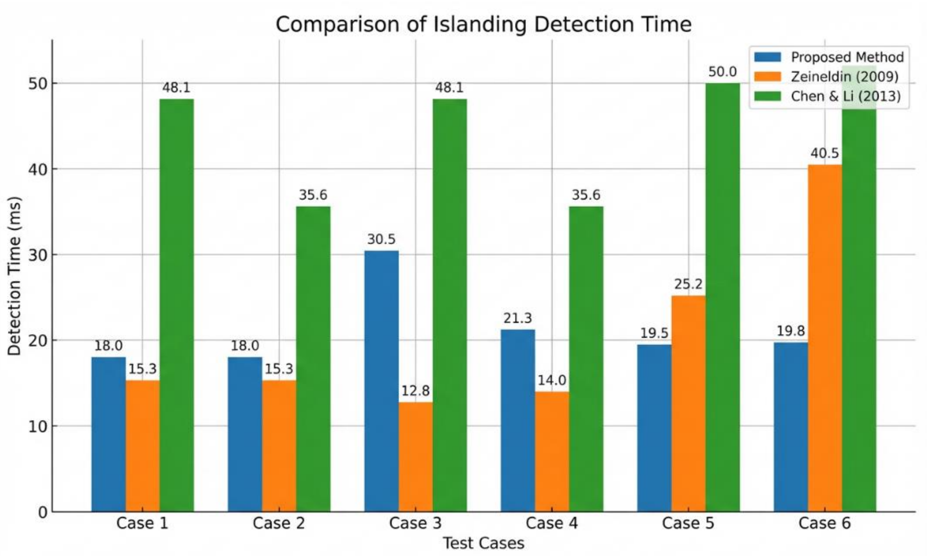

Figure 10. Voltage and Frequency Waveforms for Different Load Conditions in Cases 5 and 6

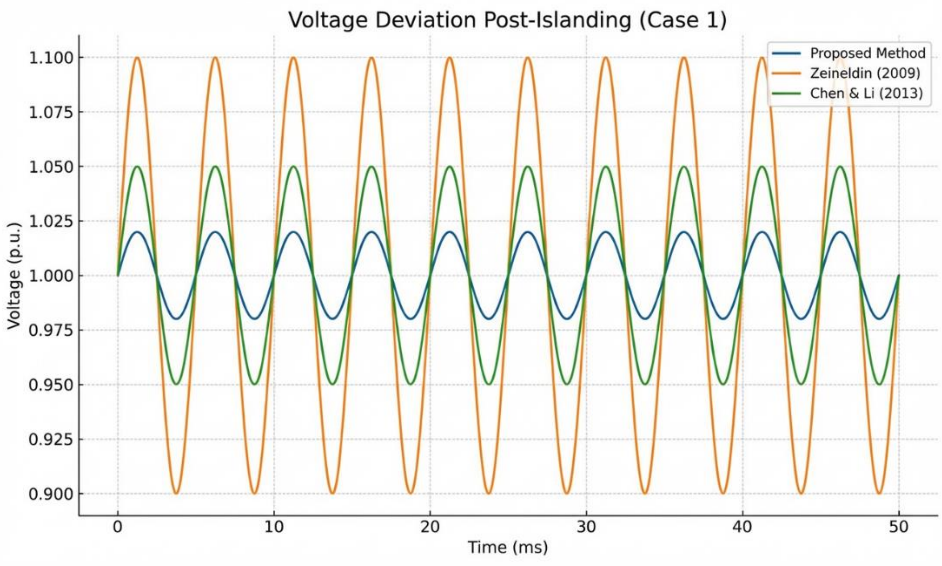

Figure 11. Voltage and Frequency Waveforms for Different Load Conditions in Cases 5 and 6

4. Discussion and Conclusion

This study provides a comparative evaluation of three distinct islanding detection methods in power systems under varying load conditions and severe network scenarios. The primary focus of the analysis was to assess detection times and voltage deviations following islanding events. The results demonstrate that the proposed method outperforms the alternative approaches. In Cases 1 and 2, the proposed method detected islanding within 18.02 milliseconds. Although the method in [19] achieved the fastest detection under conditions of reactive power mismatch, it caused significant voltage oscillations post islanding, potentially affecting local loads. In contrast, the proposed approach maintained rapid and accurate detection while minimizing voltage disturbances. For Cases 3 and 4, where load conditions were similar, the proposed method achieved detection times of 30.46 ms and 21.26 ms, respectively, whereas the method in [19] exhibited longer detection times accompanied by frequency oscillations. In Cases 5 and 6, which involved loads with negligible reactive power consumption, the proposed method still successfully detected islanding in under 20 ms, while the[19] approach required substantially longer times to trigger detection. Overall, the findings indicate that the proposed method can identify islanding events in less than 31 ms without causing significant voltage fluctuations. This demonstrates its suitability for practical applications in power systems operating under diverse load conditions and network contingencies. The study highlights the critical importance of fast and precise islanding detection techniques that minimize detection time while mitigating voltage disturbances and adverse effects on loads.

Key Advantages of the Proposed Method Compared to Existing Techniques:

- Reduction of the Non-Detection Zone (NDZ) and improved detection accuracy
- Islanding detection time consistently below 31 milliseconds
- Minimization of post-islanding voltage fluctuations
- Mitigation of negative impacts on power quality and system reliability
- Stable performance under load variations and fluctuations in network voltage and frequency

Furthermore, the GMM-based load characterization demonstrates robustness to moderate deviations from the Gaussian assumption, as evidenced by sensitivity analyses and initialization stability tests. This robustness supports reliable operation in practical distribution systems with diverse load types and increasing renewable integration. Based on these results, the proposed method emerges as a fast, accurate, and resilient solution for islanding detection in distribution systems with distributed generation.

References

[1] Arif, A., Imran, K., Cui, Q., & Weng, Y. (2021). Islanding detection for inverter-based distributed generation using unsupervised anomaly detection. *IEEE Access, 9*, 90947–90963.

[2] Hussain, A., Mirza, S., & Kim, C.-H. (2023). Islanding detection and classification of non-islanding disturbance in multi-distributed generation power system using deep neural networks. *Electric Power Systems Research, 224*, 109807.

[3] Nsaif, Y. M., Lipu, M. H., Hussain, A., Ayob, A., & Yusof, Y. (2023). Island detection for grid connected photovoltaic distributed generations via integrated signal processing and machine learning approach. *International Journal of Electrical Power & Energy Systems, 154*, 109468.

[4] Hussain, A., Kim, C.-H., & Mehdi, A. (2021). A comprehensive review of intelligent islanding schemes and feature selection techniques for distributed generation system. *IEEE Access, 9*, 146603–146624.

[5] Kharusi, K. A., Haffar, A. E., & Mesbah, M. (2023). Adaptive machine-learning-based transmission line fault detection and classification connected to inverter-based generators. *Energies, 16*(15), 5775.

[6] Shadpey, S., Chegini, M., & Ameli, M.-T. (2023). A novel pattern recognition-based plan for islanding detection in distribution systems in the presence of synchronous generator-based distributed generation resources. *Electrical Engineering, 105*(3), 1609–1627.

[7] Kim, K., Park, Y., Lee, J., & Ju, S. (2024). Control strategy of energy storage system for islanding detection based on load analysis with machine learning. *IEEE Transactions on Smart Grid, 15*(5), 4719–4730.

[8] Chandrakar, R., Dubey, R. K., & Panigrahi, B. K. (2025). Deep learning-based islanding detection method for droop-controlled grid-forming inverters. *IEEE Journal of Emerging and Selected Topics in Industrial Electronics, 6*(2), 687–698.

[9] Ezzat, A., Elnaghi, B. E., & Abdelsalam, A. A. (2021). Microgrids islanding detection using Fourier transform and machine learning algorithm. *Electric Power Systems Research, 196*, 107224.

[10] Özcanlı, A. K., & Baysal, M. (2022). A novel multi-LSTM based deep learning method for islanding detection in the microgrid. *Electric Power Systems Research, 202*, 107574.

[11] Azizi, R., & Noroozian, R. (2021). Islanding detection in distributed energy resources based on gradient boosting algorithm. *IET Renewable Power Generation, 15*(2), 436–451.

[12] Allan, O. A., & Morsi, W. G. (2021). A new passive islanding detection approach using wavelets and deep learning for grid-connected photovoltaic systems. *Electric Power Systems Research, 199*, 107437.

[13] Uzair, M., Eskandari, M., Li, L., & Zhu, J. (2022). Machine learning based protection scheme for low voltage AC microgrids. *Energies, 15*(24), 9397.

[14] Bekhradian, R., & Sanaye-Pasand, M. (2022). A comprehensive survey on islanding detection methods of synchronous generator-based microgrids: Issues, solutions and future works. *IEEE Access, 10*, 76202–76219.

[15] Aminifar, F., Teimourzadeh, S., Shahsavari, A., Savaghebi, M., & Golsorkhi, M. S. (2021). Machine learning for protection of distribution networks and power electronics-interfaced systems. *The Electricity Journal, 34*(1), 106886.

[16] Islam, M. M., Nagrial, M., Rizk, J., & Hellany, A. (2021). General aspects, islanding detection, and energy management in microgrids: A review. *Sustainability, 13*(16), 9301.

[17] Zeineldin, H. H. (2009). A Q–f droop curve for facilitating islanding detection of inverter-based distributed generation. *IEEE Transactions on Power Electronics, 24*(3), 665–673.

[18] Morgan, M. Y., et al. (2025). Isolated microgrids dominant modes prediction based on machine learning. *Protection and Control of Modern Power Systems, 10*(4), 146–156.

[19] Li, C., Cao, C., Cao, Y., Kuang, Y., Zeng, L., & Fang, B. (2014). A review of islanding detection methods for microgrid. *Renewable and Sustainable Energy Reviews, 35*, 211–220.

[20] Khamis, A., et al. (2013). A review of islanding detection techniques for renewable distributed generation systems. *Renewable and Sustainable Energy Reviews, 28*, 483–493.
[21] Golpîra, H. (2025). A data-driven based approach for islanding detection in large-scale power systems. *IEEE Transactions on Power Systems, 40*(1), 272–285.
[22] Reddy, C. R., Choi, J. H., & Pangedaiah, B. (2024). Absolute positive sequence voltage difference based passive islanding detection in microgrids. *IEEE Transactions on Industry Applications, 60*(3), 4633–4641.
[23] Chhetija, D., Rather, Z. H., & Doolla, S. (2024). Fault location identification in power islands with inverter interfaced distributed generators. *IEEE Transactions on Instrumentation and Measurement, 73*, 1–10.
[24] Mumtaz, F., Imran, K., Rehman, H., & Bukhari, S. B. A. (2024). Novel protection method for AC microgrids with multiple distributed generations using unscented Kalman filter. *Electric Power Systems Research, 230*, 110227.
[25] Shahgholian, G., Moradian, M., & Fathollahi, A. (2025). Droop control strategy in inverter-based microgrids: A brief review on analysis and application in islanded mode of operation. *IET Renewable Power Generation, 19*(1), e13186.
[26] Seyedi, M., Taher, S. A., Ganji, B., & Guerrero, J. (2021). A hybrid islanding detection method based on the rates of changes in voltage and active power for the multi-inverter systems. *IEEE Transactions on Smart Grid, 12*(4), 2800–2811.
[27] Seyedi, M., Taher, S. A., Ganji, B., & Guerrero, J. M. (2019). A hybrid islanding detection technique for inverter-based distributed generator units. *International Transactions on Electrical Energy Systems, 29*(11), e12113.
[28] Seyedi, M., Taher, S. A., & Ganji, B. (2017). Islanding detection and frequency circuit measurement by power distribution relation depending on the angle. In *Proceedings of the Conference on Electrical Power Distribution Networks (EPDC)*.
[29] Reynolds, D. A. (2009). Gaussian mixture models. In *Encyclopedia of biometrics* (pp. 659–663). Springer.
[30] Blei, D. M., & Jordan, M. I. (2006). Variational inference for Dirichlet process mixtures. *Bayesian Analysis, 1*(1), 121–143.